

Cellular automaton models of driven diffusive Frenkel-Kontorova-type systems

B. H. Wang,^{1,2,3} Y. R. Kwong,⁴ P. M. Hui,⁴ and Bambi Hu^{1,5}

¹*Department of Physics and Centre for Nonlinear Studies, Hong Kong Baptist University, Hong Kong, China*

²*Department of Modern Physics and Nonlinear Science Center, University of Science and Technology of China, Hefei 230026, Anhui, China*

³*CCAST (World Laboratory), P.O. Box 8730, Beijing 100090, China*

⁴*Department of Physics, The Chinese University of Hong Kong, Shatin, New Territories, Hong Kong, China*

⁵*Department of Physics, University of Houston, Houston, Texas 77204*

(Received 19 November 1998)

Three cellular automaton models of increasing complexity are introduced to model driven diffusive systems related to the generalized Frenkel-Kontorova (FK) models recently proposed by Braun *et al.* [Phys. Rev. E **58**, 1311 (1998)]. The models are defined in terms of parallel updating rules. Simulation results are presented for these models. The features are qualitatively similar to those models defined previously in terms of sequentially updating rules. Essential features of the FK model such as phase transitions, jamming due to atoms in the immobile state, and hysteresis in the relationship between the fraction of atoms in the running state and the bias field are captured. Formulating in terms of parallel updating rules has the advantage that the models can be treated analytically by following the time evolution of the occupation on every site of the lattice. Results of this analytical approach are given for the two simpler models. The steady state properties are found by studying the stable fixed points of a closed set of dynamical equations obtained within the approximation of retaining spatial correlations only up to two nearest-neighboring sites. Results are found to be in good agreement with numerical data. [S1063-651X(99)03807-6]

PACS number(s): 05.70.Ln, 05.45.-a, 66.30.-h, 05.60.-k

I. INTRODUCTION

The physics of driven diffusive systems has attracted much attention recently [1,2] due to their relevance to the general area of nonequilibrium statistical mechanics and their wide range of possible potential applications. In particular, the Frenkel-Kontorova (FK) model [3,4] and its generalizations [5–7] have been studied within the context of tribophysics. Braun and co-workers [8–10] studied the atomic current in one- and two-dimensional atomic systems in the presence of a periodic potential under the influence of a dc driving force within the approach of Langevin equations. In tribophysics, the driving force emerges owing to the motion of one of the two substrates separated by a thin atomic layer. The results of these studies are characterized by two features. One feature is that the system exhibits hysteresis in response to the driving force. The system jumps between low-mobility and high-mobility regimes in a hysteretic manner as a function of the driving force. Another feature is that accompanying this transition, the atoms tend to organize themselves into two types of domains consisting of atoms in states of different characters, one consisting of slowly moving (“immobile”) atoms and another consisting of “running” atoms moving with maximum speed. The latter feature resembles those in traffic flow models [11–13] in which cars may be moving at their maximum speed if they are not blocked or may be momentarily stationary if they are blocked in front.

The models studied in Refs. [8–10] are quite complicated. Attempts have been made [14] to introduce simpler models which capture the essential features. In a series of three lat-

tice gas (LG) models of increasing complexity (henceforth referred to as LG models A, B, and C), Braun *et al.* introduced probabilistic hoppings of atoms on a lattice together with the possibility of the atoms being found in one of two possible states. The underlying model (LG model A) in one dimension is that N atoms are placed in a lattice of length L corresponding to a concentration of $\rho = N/L$. The dynamics is introduced in a random and sequential fashion by randomly choosing a site at each time step and updating the system according to specific rules. The hopping to the nearest-neighboring sites of an immobile atom in a randomly chosen site is characterized by a probability $\alpha(1-\alpha)$ that an atom hops into the site in the right (left) hand side. Thus the parameter α models the effect of a driving force, and the hoppings to the right and left hand sides correspond to the effects of drift together with diffusion. Atoms in the running state always attempt to hop to the right, which is taken to be the direction of the driving force. The $\alpha=1/2$ case corresponds to vanishing bias field. The $\alpha=1$ case corresponds to the totally asymmetric exclusion model, which has been solved exactly [15]. An atom in the immobile state changes to the running state if it succeeds in hopping to the right hand side, while a running atom becomes immobile if the site to the right is occupied by an atom in the immobile state. Such transitions between the immobile and running states of an atom model the effects of damping. LG model B includes the possibility that the running atom at a randomly chosen site may change to the immobile state with probability γ prior to the motion of the atom takes place. This spon-

taneous convection from the running to the immobile state is supposed to be more important for weak driving forces. In order to capture the features of hysteresis, Braun *et al.* [14] went on to include in the basic model a majority rule in the conversion between the two states of the atoms. If the randomly chosen site is occupied by the leading atom in a compact group of r running atoms and it is blocked by a compact group of s immobile atoms in front, all the $r+s$ atoms will turn into the immobile (running) state if $r < s$ ($r \geq s$). These three models have the advantage of being easily implemented numerically by carrying out Monte Carlo simulations.

It is useful to study similar models within the context of dynamical systems. A physical consideration is that parallel updatings of the states of the atoms may be more appropriate than the sequential updatings in the LG models studied in Ref. [14]. In the present work, we propose analogous models with parallel updating rules in that all the atoms evolve in every time step according to updating rules, and hence the models become cellular automaton (CA). We performed numerical simulations on the models. Another advantage of casting the models in terms of parallel updating rules is that a more systematic analytical approach, analogous to those successfully applied to traffic flow models [16,17], may be applicable. Such an approach focuses on the time evolution on the state of each of the sites, namely, whether the site is occupied by an atom in the running or immobile state or unoccupied. In general, spatial correlations of gradually increasing spatial extent are introduced as time evolves. Equations can be written down relating the state of a site at time $t+1$ to quantities at time t . By suitably decoupling the spatial correlations, a set of coupled nonlinear equations can be obtained with the fixed point corresponding to the solution in the long-time limit. The complexity of the set of equations depends on the extent of spatial correlations retained after decoupling. The approach has the advantage that it gives the fraction of running atoms in the steady state together with other spatial correlation functions. As an illustration of the general idea of the approach, we study models A and B with parallel updating rules and results are found to be in reasonable agreement with numerical simulations within the approximation of retaining correlations up to two sites. The present work, therefore, complements that of Braun *et al.* [14] and suggests an alternative way of studying the various models proposed within the context of tribology.

The plan of the paper is as follows. In Sec. II, we define the modified models with parallel updating rules and present the results obtained by numerical simulations. Section III reports results of our analytical calculations on models A and B. Results are compared with numerical simulations. We summarize the results in Sec. IV.

II. MODELS AND NUMERICAL RESULTS

A. Model A

We consider N atoms on a one-dimensional lattice of L sites with periodic boundary condition. Following the basic lattice gas model [14], we modify the rules such that parallel updating is incorporated. The updating rules are the following.

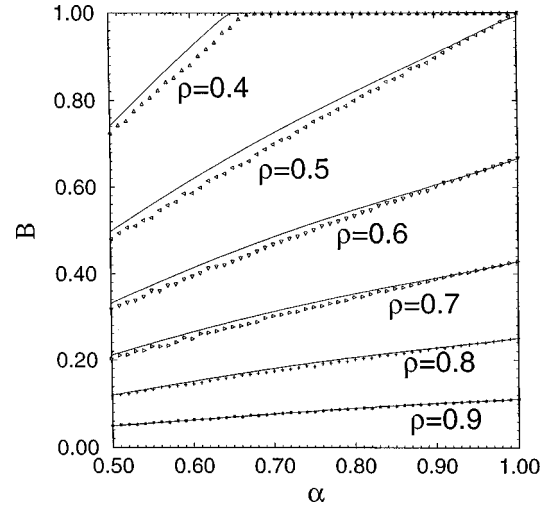


FIG. 1. The fraction B of atoms in the running state for model A in the long-time limit as a function of the dimensionless external biasing parameter α for different values of the concentration of atoms ρ . This dimensionless quantity is referred to as the mobility, as it gives the number of sites hopped per atom per time step. The symbols are numerical data, and the solid lines are results obtained by invoking the decoupling scheme in the analytical approach discussed in the text.

Rule A1. If the i th site on the lattice at time t is occupied by an immobile atom, it has a probability α to be in the advancing immobile state, i.e., the state that favors forward biasing and a probability $1 - \alpha$ to be in the retreating immobile state, i.e., the state that favors backward hopping. An advancing immobile atom can either hop into the *empty* $(i+1)$ th site and become a running atom if the $(i+2)$ th site is *not* occupied by a retreating atom or be blocked by an atom occupying the $(i+1)$ th site without changing its state, while a retreating atom can either hop into the *empty* $(i-1)$ th site and stay in the immobile state if the $(i-2)$ th site is *not* occupied by a running or an advancing immobile atom or be blocked by an atom occupying the $(i-1)$ th site without changing its state.

Rule A2. If the i th site on the lattice at time t is occupied by a running atom, it can move to the *empty* $(i+1)$ th site if the $(i+2)$ th site is *not* occupied by a retreating atom or stay at the i th site and remain in the running state if it is blocked by a running atom or change to the immobile state if it is blocked by an immobile atom at the $(i+1)$ th site.

Rule A3. If the i th site on the lattice at time t is empty and is sandwiched between a running or advancing immobile atom at the $(i-1)$ th site and a retreating immobile atom at the $(i+1)$ th site, then the atoms at the two neighboring sites are equally probable to hop into the i th site according to rules A1 and A2. The atom that fails to hop at that time step will remain in its original state.

Model A thus represents a modification of the LG model A in Ref. [14] with parallel updating rules. The quantity of interest is the fraction B of atoms in the running state in the long-time limit. This dimensionless quantity also reflects the number of sites hopped per atom per time step in the long time limit. Following Ref. [14], B is also referred to as the

mobility. We have carried out numerical simulations on model A. Figure 1 shows the dependence of the mobility B as a function of the drift parameter α for different concentrations of atoms ρ . Note that only the range $1/2 < \alpha \leq 1$ corresponding to a biased field to the right hand side is shown, although the range $0 < \alpha < 1/2$ can also be studied taking model A as a CA model in its own right. To illustrate the basic features of the model, we have performed numerical simulations on systems with $L = 1000$. Typically, about 2000 time steps are sufficient for approaching the long-time limit. The mobility B is obtained simply by counting the fraction of running atoms in the long-time limit. For $\alpha < 1$, an average over 50 random initial configurations are performed. For $\alpha > 1/2$, $B = 1$ for $\rho < 0.32$. For $0.32 < \rho < 1/2$, the mobility B becomes unity at some critical value $\alpha_c(\rho)$. For $\rho > 1/2$, the concentration is sufficiently high so that $B < 1$ for all values of α .

The particular point of $\alpha = 1$ deserves further discussion. It is found that for $\rho > 1/2$, the mobility B at $\alpha = 1$ in the long time limit depends on the initial condition. The results at $\alpha = 1$ shown in Fig. 1 correspond to $B = (1 - \rho)/\rho$, which are obtained by using the initial configuration in which all the atoms are immobile. For arbitrary initial configurations at $\alpha = 1$, B is found to lie within the range $(1 - \rho)/\rho \leq B \leq 1$. Similar results are obtained in our analytical approach, discussed in the next section, by treating the model as a dynamical system.

B. Model B

Model A forms the basic CA model for further modifications. In particular, while an irreversible transition into the running state for an isolated atom is strongly favorable in the high-field limit ($\alpha \approx 1$), it is possible for a running atom to convert spontaneously to the immobile state in the weak-field case. Following the LG model B in Ref. [14], we introduce the following rule in addition to the rules A1, A2, and A3 stated above:

Rule B1. Before the updating rules A1, A2, and A3 are applied in each time step, every atom in the running state has a probability γ to change its state to the immobile state and a probability $1 - \gamma$ to remain in the running state. After this consideration, all the atoms on the lattice evolve according to the rules A1, A2, and A3.

Rules B1, A1, A2, and A3 define the CA model B. While α tends to lead to a larger fraction of running atom, the parameter γ counteracts the effect and tends to increase the number of atoms in the immobile state. Hence the mobility B is generally lower for $\gamma \neq 0$ cases than the $\gamma = 0$ case for the same value of α . Figure 2 shows the values of B as a function of α for different values of γ with the concentration fixed at $\rho = 0.4$, which corresponds to a concentration at which the atoms are isolated if they are uniformly distributed on the lattice. Note that the mobilities converge to unity at $\alpha = 1$ for different values of γ . Only when $\gamma = 0$ will the mobility becomes unity for $\alpha_c < \alpha \leq 1$. The results shown are typical for $\rho < 1/2$. Figure 3 shows the results for $\rho = 0.6$, which corresponds to a concentration at which there are always some atoms with nearest neighbors if they are uniformly distributed on the lattice. In this case, $B < 1$ for all

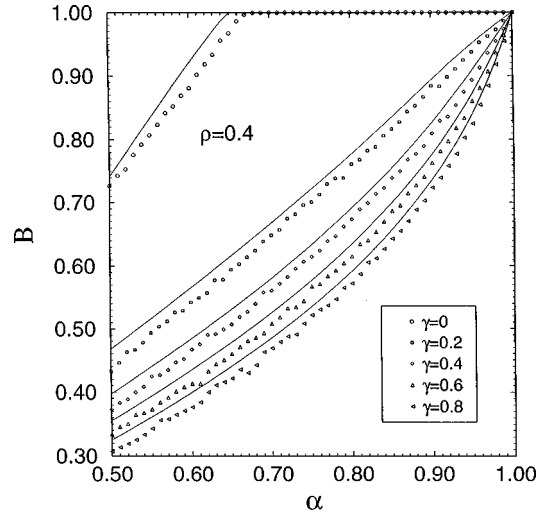


FIG. 2. The fraction B of atoms in the running state for model B in the long-time limit as a function of the dimensionless biasing parameter α for different values of the parameter γ at fixed concentration $\rho = 0.4$. The symbols are numerical results, and the solid lines are results obtained by invoking the decoupling scheme. Results are typical of those for $\rho < 1/2$.

values of $1/2 < \alpha < 1$ and $0 \leq \gamma \leq 1$. The mobilities converge to the same value for different values of γ at $\alpha = 1$. For $\gamma = 0$, model B reduces to model A and the mobility B lies in the range $(1 - \rho)/\rho \leq B \leq 1$ with the precise value depending on the initial condition.

C. Model C

Following the LG model C in Ref. [14], further modifications can be made by taking into account the influence of the state of the surrounding atoms on that of a single atom, i.e., the ‘‘crowding effect.’’ The modifications involve the considerations of the jamming of a running block of atoms (i.e., a compact group of nearest-neighboring atoms in the running state) by an immobile block of atoms (i.e., a compact group

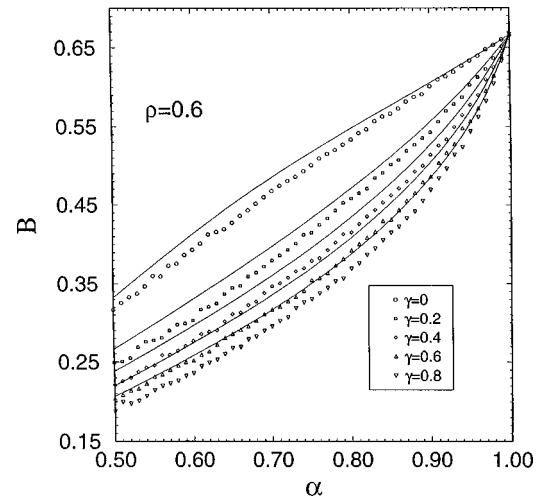


FIG. 3. The fraction B of atoms in the running state for model B in the long-time limit as a function of the dimensionless biasing parameter α for different values of the parameter γ at fixed concentration $\rho = 0.6$. The symbols are numerical results, and the solid lines are results obtained by invoking the decoupling scheme. Results are typical of those for $\rho > 1/2$.

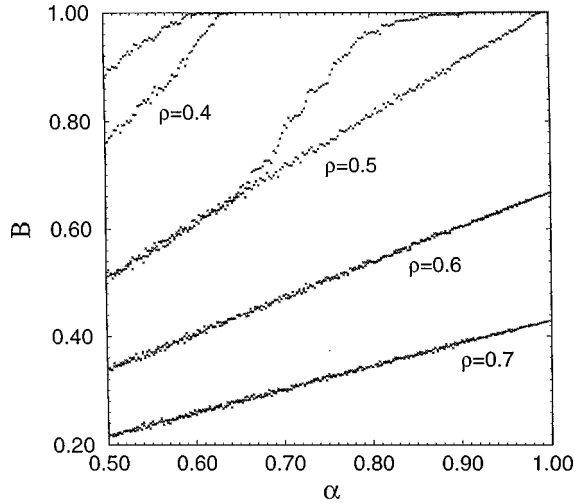


FIG. 4. The fraction B of atoms in the running state for model C in the long-time limit as a function of the dimensionless biasing parameter α for different values of the concentration ρ . The parameter γ_0 is taken to be 10^{-5} . Results are typical for those with $\gamma_0 \approx 0$. Hysteresis in the mobility is observed for $\rho \leq 1/2$.

of atoms in the immobile state). If these two adjacent blocks of atoms are sandwiched between two empty sites at the two ends, the state of *all* the atoms will then follow that of the larger block. This rule will be referred to as the majority rule. Furthermore, since the spontaneous transition of atoms in the running state to the immobile state should be suppressed by an increasingly stronger forward bias, the parameter γ should be α dependent. We impose the relation [14] $\gamma = \gamma_0(1 - \alpha)^2$ on the parameter γ , where γ_0 is a model parameter. Hence the updating rules for model C can be stated explicitly as below.

Rule C1. At a certain time step, if the $(i-r+1)$ th site to the i th site is *all* occupied by running atoms and the $(i+1)$ th site to the $(i+s)$ th site is *all* occupied by immobile atoms together with the condition that the $(i-r)$ th site and $(i+s+1)$ th site be empty, then in the case of $r \geq s$ ($r < s$), *all* the $r+s$ atoms become running (immobile). Immediately after the changes, the states of the sites are then updated according to the rules of model B with $\gamma = \gamma_0(1 - \alpha)^2$.

Rule C1 together with model B define the CA model C. Figure 4 shows typical results for the mobility B as a function of α for different values of ρ with γ_0 taking on a value close to 0. It is observed that the results look very similar to that of model A except for the presence of *hysteresis*, a characteristic feature of the FK model [14], for $\rho \leq 1/2$. The values of B obtained by gradually increasing α from $\alpha = 0.5$ to $\alpha = 1$ are generally smaller than those obtained by gradually decreasing α from $\alpha = 1$, and the difference between the mobilities for increasing and decreasing bias fields at a particular value of α increases with α as observed in the LG model in Ref. [14].

The hysteresis, which is absent from models A and B, observed for $\rho \leq 1/2$ in model C originates from the interactions between compact blocks of running atoms and those of the immobile atoms. To understand qualitatively the origin of such irreversible behavior, we consider the probability of

finding the configuration in which a compact block of r running atoms is immediately followed by a compact block of s immobile atoms with an empty site at both ends. By definition the density of running atoms on the lattice is ρB and the density of immobile atoms is $\rho(1-B)$. The probability of having a compact block of r running atoms immediately followed by a compact block of s immobile atoms is thus $[\rho B(t)]^r [\rho(1-B(t))]^s$, where $B(t)$ is the fraction of running atom at a particular instant. Therefore, the probability of finding the desired configuration with an empty site at both ends is $P = (1-\rho)^2 \rho^{r+s} B(t)^r [1-B(t)]^s$. We focus on the upper branch of the hysteresis obtained when α is lowered from $\alpha = 1$. In this case, the system evolves from an initial configuration with $B \approx 1$, which is attainable *only* for $\rho \leq 1/2$ at $\alpha = 1$. For values of B close to unity, the probability P is larger for $r > s$ than for $r < s$. This asymmetry implies that it is more probable to find blocks with more running atoms than immobile atoms. By rule C1, the asymptotic state will consist of more running atoms and hence a larger value of B . Therefore, the asymptotic values of B are generally larger if one starts with an initial configuration with a larger number of running atoms. This sensitivity to the initial configurations leads to the hysteresis observed in the fraction of running atoms as α is gradually increased and decreased.

III. ANALYTICAL APPROACH

The CA models with parallel updating rules have the advantage that they can be treated analytically within the context of dynamical systems. The general idea is to establish the time evolution equations for the state on each site of the lattice. The equations, in general, involve spatial correlation functions. With suitable approximations typically involving proper decoupling of the correlations, a closed set of dynamical equations can be obtained. Such a set of equations can be treated as a dynamical mapping between quantities at time $t+1$ and those at time t . Hence, following standard approaches in dynamical systems, the solution in the long-time limit can be found by studying the fixed points (attractors) of the set of equations. Such an approach has been successfully developed for traffic flow models [16,17] in which the cars, which are analogous to the atoms in the present models, can only move in one direction without backward diffusion movements. To illustrate the idea, we apply the approach to study the modified CA models. It turns out that for models A and B, reasonably good agreement with numerical simulations can be obtained by retaining spatial correlations involving two neighboring sites only. Application of the method to model C is difficult due to the built-in long spatial correlations in the majority rule of the model, and hence results are only reported for models A and B.

A. Model A

Although one can treat model B directly and obtain results of model A by setting $\gamma = 0$, it is, however, illustrative to treat the simpler model A first. We denote the states of the i th site at time t by the following set of Boolean variables:

$$R_i(t) = \begin{cases} 1 & \text{if the } i \text{ th site at time } t \text{ is occupied by a running atom,} \\ 0 & \text{otherwise,} \end{cases} \quad (1)$$

$$I_i(t) = \begin{cases} 1 & \text{if the } i \text{ th site at time } t \text{ is occupied by an immobile atom,} \\ 0 & \text{otherwise,} \end{cases} \quad (2)$$

$$S_i(t) \equiv R_i(t) + I_i(t) = \begin{cases} 1 & \text{if the } i \text{ th site at time } t \text{ is occupied,} \\ 0 & \text{otherwise.} \end{cases} \quad (3)$$

Obviously, these variables satisfy the relationships $R_i(t)R_i(t) = R_i(t)S_i(t) = R_i(t)$, $I_i(t)I_i(t) = I_i(t)S_i(t) = I_i(t)$, $S_i(t)S_i(t) = S_i(t)$, $R_i(t)R_i(t) = I_i(t)I_i(t) = 0$, and $R_i(t)I_i(t) = R_i(t)S_i(t) = I_i(t)S_i(t) = 0$. Here $R_i(t)$ represents the conjugate to $R_i(t)$ given by $\overline{R_i(t)} = 1 - R_i(t)$, with similar definitions for $S_i(t)$ and $I_i(t)$.

In order to represent whether an immobile atom is advancing or retreating at a certain time step t , we define a Boolean variable $\theta_{i,t}(f)$ at the i th site at time t such that

$$\theta_{i,t}(f) = \begin{cases} 1 & \text{with probability } f, \\ 0 & \text{with probability } (1-f). \end{cases} \quad (4)$$

Thus the term $\theta_{i,t}(\alpha)I_i(t)$ represents the probability that the i th site at time t is occupied by an advancing immobile atom, while the term $\overline{\theta_{i,t}(\alpha)}I_i(t)$ represents the probability that the i th site at time t is occupied by a retreating atom. Here $\overline{\theta_{i,t}(\alpha)}$ denotes the conjugate of $\theta_{i,t}(\alpha)$, i.e., $\overline{\theta_{i,t}(\alpha)} \equiv 1 - \theta_{i,t}(\alpha)$. It follows that $\theta_{i,t}(\alpha)\overline{\theta_{i,t}(\alpha)} = \theta_{i,t}(\alpha)$ and $\overline{\theta_{i,t}(\alpha)}\theta_{i,t}(\alpha) = 0$. Similarly, in order to represent whether an advancing or an immobile atom can hop into the empty site sandwiched between the two atoms at a certain time step, another Boolean variable $\eta_{i,t}(f)$ defined exactly the same as $\theta_{i,t}(f)$ is introduced with $f=1/2$. With this, the factor $\eta_{i,t}(1/2)R_i(t)\overline{S_{i+1}(t)}[\overline{\theta_{i+2,t}(\alpha)}I_{i+2}(t)]$ represents, for example, the probability that the advancing running atom at the i th site can hop successfully into the $(i+1)$ th site at time t . Note that the two Boolean variables $\theta_{i,t}(f)$ and $\eta_{i,t}(f)$ are statistically uncorrelated.

We study the time evolution of the variables $R_i(t)$ and $I_i(t)$, i.e., we seek the variables $R_i(t+1)$ and $I_i(t+1)$ as a function of quantities at time t . Focusing on $R_i(t+1)$, there are various ways in which the situation at time t affects $R_i(t+1)$. From the rules A1 and A2, a running or an advancing immobile atom occupying the $(i-1)$ th site at time t will hop into the empty i th site if the $(i+1)$ th site is not occupied by a retreating immobile atom. At the next time step, the $(i-1)$ th site will become empty, while the i th site will be occupied by a running atom. This leads to a contribution to $R_i(t+1)$ of the form

$$\begin{aligned} & [R_{i-1}(t) + \theta_{i-1,t}(\alpha)I_{i-1}(t)][\overline{S_i(t)}][\overline{\theta_{i+1,t}(\alpha)}I_{i+1}(t) \\ & + \overline{S_{i+1}(t)} + R_{i+1}(t)]. \end{aligned}$$

The three brackets express the conditions on the $(i-1)$ th, i th, and $(i+1)$ th sites at time t , respectively. The three terms

in the last set of brackets is equivalent to saying that the $(i+1)$ th site is not occupied by a retreating immobile atom at time t .

The second contribution to $R_i(t+1)$ comes from the situation in which the $(i+1)$ th site is occupied by a retreating immobile atom. In this case, rule A3 leads to another probabilistic event. This situation contributes a term to $R_i(t+1)$ of the form

$$\begin{aligned} & \eta_{i-1,t}(\frac{1}{2})[R_{i-1}(t) + \theta_{i-1,t}(\alpha)I_{i-1}(t)][\overline{S_i(t)}] \\ & \times [\overline{\theta_{i+1,t}(\alpha)}I_{i+1}(t)], \end{aligned}$$

which denotes the probability that the atom at the $(i-1)$ th site succeeded in moving forward into the empty i th site and became a running atom. The first factor $\eta_{i-1,t}(\frac{1}{2})$ follows from rule A3 as the atoms at the $(i-1)$ th and $(i+1)$ th sites are equally probable to hop into the i th site.

Another contribution comes in when the i th site is occupied by a running atom, the $(i+1)$ th site is empty, the $(i+2)$ th site is occupied by a retreating immobile atom, and that the retreating atom succeeded in hopping back onto the $(i+1)$ th site in the process. In this situation, the running atom will stay on the i th site at the next time step. This contributes a term.

$$\overline{\eta_{i,t}(\frac{1}{2})[R_i(t)][\overline{S_{i+1}(t)}][\overline{\theta_{i+2,t}(\alpha)}I_{i+2}(t)]}$$

to $R_i(t+1)$, with the brackets expressing the conditions at the i th, $(i+1)$ th, and $(i+1)$ th sites. A fourth contribution comes from the situation that a running atom at the i th site is blocked by another running atom at the $(i+1)$ th site and it gives a term

$$R_i(t)R_{i+1}(t)$$

to $R_i(t+1)$ according to rule A2.

Collecting all four contributions to $R_i(t+1)$, we have

$$\begin{aligned} R_i(t+1) = & [R + \theta(\alpha)I]_{i-1,t}[\overline{S}]_{i,t}[\theta(\alpha)I + \overline{S} + R]_{i+1,t} \\ & + [\eta(\frac{1}{2})(R + \theta(\alpha)I)]_{i-1,t}[\overline{S}]_{i,t}[\overline{\theta(\alpha)}I]_{i+1,t} \\ & + [\eta(\frac{1}{2})R]_{i,t}[\overline{S}]_{i+1,t}[\overline{\theta(\alpha)}I]_{i+2,t} \\ & + [R]_{i,t}[R]_{i+1,t}, \end{aligned} \quad (5)$$

which is a time evolution equation for $R_i(t+1)$ in that all the quantities on the right-hand side are evaluated at time t . Note that we have simplified the notations so that all the quantities

inside a set of squared brackets are to be evaluated at the position and time indicated as subscripts outside the brackets.

A similar argument can be carried out for $I_i(t+1)$, although the analysis is slightly more complicated than the case of $R_i(t+1)$. Rule A1 states that if the $(i-1)$ th site is not occupied by a running or an advancing immobile atom, then the retreating immobile atom at the $(i+1)$ th site can hop into the empty i th site deterministically. This contributes to $I_i(t+1)$ a term of the form

$$\overline{[\theta_{i-1}(t)I_{i-1}(t) + S_{i-1}(t)]} \overline{[S_i(t)]} \overline{[\theta_{i+1,t}(\alpha)I_{i+1}(t)]},$$

where the terms in the first set of squared brackets is equivalent to saying that the $(i-1)$ th site is not occupied by a running or an advancing immobile atom.

Rule A3 comes into consideration through various situations. If the $(i-1)$ th site is occupied by a running or an advancing immobile atom, the retreating immobile atom at the $(i+1)$ th site still has half a chance to hop into the empty i th site and contributes a term

$$\overline{\eta_{i-1,t}(\frac{1}{2})} \overline{[R_{i-1}(t) + \theta_{i-1,t}(\alpha)I_{i-1}(t)]} \overline{[S_i(t)]} \\ \times \overline{[\theta_{i+1,t}(\alpha)I_{i+1}(t)]}$$

to $I_i(t+1)$. Note that when an *advancing* immobile atom *fails* to hop forward, it will stay at the site and remain immobile. In this case, an advancing immobile atom located at the i th site at time t will still be there at time $t+1$ contributing a term to $I_i(t+1)$ of the form

$$\overline{[\eta_{i,t}(\frac{1}{2})\theta_{i,t}(\alpha)I_i(t)]} \overline{[S_{i+1}(t)]} \overline{[\theta_{i+2,t}(\alpha)I_{i+2}(t)]}.$$

An analogous situation arises when the running or advancing immobile atom located at the $(i-2)$ th site succeeded in hopping into the empty $(i-1)$ th site, leaving a retreating immobile atom at the i th site. This contributes a term to $I_i(t+1)$ as

$$\overline{\eta_{i-2,t}(\frac{1}{2})} \overline{[R_{i-2}(t) + \theta_{i-2,t}(\alpha)I_{i-2}(t)]} \overline{[S_{i-1}(t)]} \\ \times \overline{[\theta_{i,t}(\alpha)I_i(t)]}.$$

Blocking by atoms in the nearest-neighboring sites contributes the following terms. If an advancing immobile atom at the i th site is blocked by an atom at the $(i+1)$ th site or a retreating immobile atom is blocked by an atom at the $(i-1)$ th site, the state of the i th site at time $t+1$ remains to be immobile. These two terms in $I_i(t+1)$ are represented by $[\theta_{i,t}(\alpha)I_i(t)]S_{i+1}(t) + S_{i-1}(t)[\theta_{i,t}(\alpha)I_i(t)]$. Finally, according to rule A2, a term $R_i(t)I_{i+1}(t)$ in $I_i(t+1)$ arises from the blocking of a running atom by an immobile atom.

Collecting all the contributions to $I_i(t+1)$, we have

$$I_i(t+1) = \overline{[\theta(\alpha)I + \bar{S} + \eta(\frac{1}{2})(R \\ + \theta(\alpha)I)]_{i-1,t}} \overline{[\bar{S}]_{i,t}} \overline{[\theta(\alpha)I]_{i+1,t}} \\ + \overline{[\eta(\frac{1}{2})\theta(\alpha)I]_{i,t}} \overline{[\bar{S}]_{i+1,t}} \overline{[\theta(\alpha)I]_{i+2,t}} \\ + \overline{[\eta(\frac{1}{2})(R + \theta(\alpha)I)]_{i-2,t}} \overline{[\bar{S}]_{i-1,t}} \overline{[\theta(\alpha)I]_{i,t}}$$

$$+ \overline{[\theta(\alpha)I]_{i,t}} \overline{[S]_{i+1,t}} + \overline{[S]_{i-1,t}} \overline{[\theta(\alpha)I]_{i,t}} \\ + \overline{[R]_{i,t}} \overline{[I]_{i+1,t}}. \quad (6)$$

Equations (5) and (6) can be used to compute the time evolution of the mobility of the system and the spatial averages of the products of different combinations of the state variables defined on the same or neighboring sites.

The mobility $B(t)$ at time t , i.e., the fraction of atoms in the running state at time t , can be expressed in terms of $R_i(t)$ as

$$B(t) \equiv \frac{1}{N} \sum_i R_i(t) = \frac{1}{\rho} \langle R_i(t) \rangle, \quad (7)$$

where $\langle \dots \rangle \equiv 1/N \sum_i (\dots)$ is the spatial average of the quantity concerned over the system. It follows that $B(t+1) = (1/\rho) \langle R_i(t+1) \rangle$. Making use of the expression for $R_i(t+1)$ in terms of quantities at time t given by Eq. (5), the mobility at time $t+1$ can be expressed in terms of spatial averages involving strings of up to three neighboring sites at time t . This gives

$$B(t+1) = [\alpha \langle ROI \rangle_t + \alpha^2 \langle IOI \rangle_t + \langle R00 \rangle_t + \alpha \langle IO0 \rangle_t + \langle ROR \rangle_t \\ + \alpha \langle IOR \rangle_t] + \frac{1-\alpha}{2} [\langle ROI \rangle_t + \alpha \langle IOI \rangle_t] \\ + \frac{1-\alpha}{2} \langle ROI \rangle_t + \langle RR \rangle_t. \quad (8)$$

For simplicity, we write the spatial averages at time t as $\langle \dots \rangle_t$, and express the strings of neighboring sites in order from left to right. We use the symbol ‘‘0’’ to denote an empty site or \bar{S} . For example, $\langle ROI \rangle_t$ implies counting the strings of neighboring sites with a running atom on the left and an immobile atom on the right with an empty site in between over the system at time t . The prefactors resulted from the fact that the spatial averages of the Boolean variable $\theta(\alpha)$ (or its conjugate) survive with a probability α (or $1-\alpha$). Similarly, $\eta(1/2)$ survives with probability $1/2$ under averaging. Thus, the term $\alpha \langle ROI \rangle_t$ comes from the average $\langle R0\theta(\alpha)I \rangle_t$. Noting that $S_i(t) + \bar{S}_i(t) = R_i(t) + I_i(t) + \bar{S}_i(t) = 1$, we have

$$B(t+1) = \frac{1}{\rho} \left[\langle RR \rangle_t + \langle R0 \rangle_t + \alpha \langle IO \rangle_t - \alpha \frac{1-\alpha}{2} \langle IOI \rangle_t \right]. \quad (9)$$

Equation (9) is an exact expression for $B(t+1)$ in terms of quantities evaluated at time t . In order to proceed, we write down the evolution equation for the spatial averages on the right-hand side of Eq. (9). Obviously, iterating the equations backward in time gives terms involving longer strings of neighboring sites and hence longer spatial correlations. To close the set of equations, a decoupling scheme retaining spatial averages involving two neighboring sites is invoked. The set of equations can then be treated as a dynamical system. The fixed points of the equations then give the results corresponding to the long time limit.

To treat the system analytically, we decouple the term $\langle IOI \rangle_t$ in Eq. (9) into products of averages involving two

neighboring sites, i.e., $\langle IOI \rangle_t \approx \langle IO \rangle_t \langle OI \rangle_t / (1 - \rho)$, where $1 - \rho = \langle 0 \rangle_t$ is the probability of finding an empty site [18]. With this approximation, Eq. (9) becomes

$$B(t+1) = \frac{1}{\rho} \left[\langle RR \rangle_t + \langle R0 \rangle_t + \alpha \langle IO \rangle_t - \alpha \frac{1 - \alpha}{2} \frac{\langle IO \rangle_t \langle OI \rangle_t}{1 - \rho} \right]. \quad (10)$$

With the four variables R , I , S , and \bar{S} , a total of 16 two-site spatial averages can be formed, among which four of them can be chosen to be independent. We choose the independent spatial averages to be $\langle RR \rangle_t$, $\langle RI \rangle_t$, $\langle IR \rangle_t$, and $\langle II \rangle_t$. The other two-site averages are related through

$$\begin{aligned} \langle R1 \rangle_t &= \langle RR \rangle_t + \langle RI \rangle_t, \\ \langle 1R \rangle_t &= \langle RR \rangle_t + \langle IR \rangle_t, \\ \langle I1 \rangle_t &= \langle IR \rangle_t + \langle II \rangle_t, \\ \langle 1I \rangle_t &= \langle RI \rangle_t + \langle II \rangle_t, \\ \langle R0 \rangle_t &= \rho B(t) - \langle R1 \rangle_t, \\ \langle I0 \rangle_t &= \rho [1 - B(t)] - \langle I1 \rangle_t, \\ \langle 0R \rangle_t &= \rho B(t) - \langle 1R \rangle_t, \\ \langle 0I \rangle_t &= \rho [1 - B(t)] - \langle 1I \rangle_t, \\ \langle 01 \rangle_t &= \rho - \langle R1 \rangle_t - \langle I1 \rangle_t, \\ \langle 10 \rangle_t &= \langle 01 \rangle_t, \end{aligned}$$

$$\langle 00 \rangle_t = 1 - \rho - \langle 01 \rangle_t,$$

$$\langle 11 \rangle_t = \langle I1 \rangle_t + \langle R1 \rangle_t, \quad (11)$$

where “1” represents an occupied site regardless of the character of the atom. Using $\langle RR \rangle_{t+1} = \langle R_i(t+1)R_{i+1}(t+1) \rangle$ and Eq. (5) for $R_i(t+1)$ and $R_{i+1}(t+1)$, we have

$$\begin{aligned} \langle RR \rangle_{t+1} &= \langle RRR \rangle_t + \frac{1 - \alpha}{2} \langle RROI \rangle_t + \langle R0RR \rangle_t + \alpha \langle IORR \rangle_t \\ &+ \frac{1 - \alpha}{2} [\langle R0ROI \rangle_t + \alpha \langle IOROI \rangle_t]. \end{aligned} \quad (12)$$

To make the approximation self-consistent, we invoke the decoupling scheme and retaining spatial averages involving no more than two sites: we have

$$\begin{aligned} \langle RR \rangle_{t+1} &= \frac{\langle RR \rangle_t^2}{\rho B(t)} + \frac{\langle RR \rangle_t}{(1 - \rho)\rho B(t)} \\ &\times \left\{ \frac{1 - \alpha}{2} \langle R0 \rangle_t \langle OI \rangle_t + \langle 0R \rangle_t [\langle R0 \rangle_t + \alpha \langle IO \rangle_t] \right\} \\ &+ \frac{1 - \alpha}{2} \frac{\langle R0 \rangle_t \langle OR \rangle_t \langle OI \rangle_t}{(1 - \rho)^2 \rho B(t)} [\langle R0 \rangle_t + \alpha \langle IO \rangle_t]. \end{aligned} \quad (13)$$

Similarly, for $\langle RI \rangle_{t+1}$, $\langle IR \rangle_{t+1}$, and $\langle II \rangle_{t+1}$, we obtain, after decoupling,

$$\begin{aligned} \langle RI \rangle_{t+1} &= \frac{\langle RR \rangle_t \langle RI \rangle_t}{\rho B(t)} + \frac{1 - \alpha}{1 - \rho} \langle OI \rangle_t \left[\langle R0 \rangle_t + \frac{\alpha}{2} \langle IO \rangle_t \right] \\ &+ \frac{1}{1 - \rho} [\langle R0 \rangle_t + \alpha \langle IO \rangle_t] \left\{ \frac{\langle OR \rangle_t \langle RI \rangle_t}{\rho B(t)} + \frac{1 - \alpha}{1 - \rho} \langle 00 \rangle_t \langle OI \rangle_t + \alpha \frac{\langle OI \rangle_t \langle I1 \rangle_t}{\rho [1 - B(t)]} + \frac{\alpha}{2} \frac{1 - \alpha}{1 - \rho} \frac{\langle OI \rangle_t^2 \langle IO \rangle_t}{\rho [1 - B(t)]} \right\}, \end{aligned} \quad (14)$$

$$\langle IR \rangle_{t+1} = \frac{1}{\rho B(t)} \left[\langle RR \rangle_t + \frac{1 - \alpha}{2(1 - \rho)} \langle R0 \rangle_t \langle IO \rangle_t \right] \left\{ \alpha \langle IR \rangle_t + (1 - \alpha) \frac{\langle I1 \rangle_t \langle IR \rangle_t}{\rho [1 - B(t)]} + \frac{1 - \alpha}{2(1 - \rho)} \frac{\langle OI \rangle_t \langle IR \rangle_t}{\rho [1 - B(t)]} \right\}, \quad (15)$$

$$\begin{aligned} \langle II \rangle_{t+1} &= (1 - \alpha) [\langle RI \rangle_t + \alpha \langle II \rangle_t] + \frac{\alpha}{2} \frac{1 - \alpha}{1 - \rho} \langle OI \rangle_t \langle IO \rangle_t + \frac{\alpha}{\rho B(t)} \langle RI \rangle_t \langle IR \rangle_t + (1 - \alpha)^2 \frac{\langle I1 \rangle_t \langle II \rangle_t}{\rho [1 - B(t)]} + \alpha \left[\frac{\langle RI \rangle_t \langle I1 \rangle_t}{\rho [1 - B(t)]} \right. \\ &+ \alpha \frac{\langle II \rangle_t \langle I1 \rangle_t}{\rho [1 - B(t)]} \left. \right] + \frac{(1 - \alpha)^2}{1 - \rho} \frac{\langle OI \rangle_t \langle I1 \rangle_t \langle IO \rangle_t}{\rho [1 - B(t)]} + \frac{1 - \alpha}{\rho B(t)} \frac{\langle RI \rangle_t \langle I1 \rangle_t \langle IR \rangle_t}{\rho [1 - B(t)]} + \alpha (1 - \alpha) \frac{\langle I1 \rangle_t \langle II \rangle_t \langle I1 \rangle_t}{\rho^2 [1 - B(t)]^2} \\ &+ \frac{\alpha}{2} \frac{1 - \alpha}{1 - \rho} \frac{\langle IO \rangle_t \langle OI \rangle_t}{\rho^2 [1 - B(t)]^2} [\langle RI \rangle_t + \alpha \langle II \rangle_t] + \frac{(1 - \alpha)^2}{2(1 - \rho)} \frac{\langle OI \rangle_t \langle II \rangle_t}{\rho [1 - B(t)]} [\langle R0 \rangle_t + \alpha \langle IO \rangle_t] + \frac{1}{2} \left(\frac{1 - \alpha}{1 - \rho} \right)^2 \frac{\langle OI \rangle_t^2 \langle IO \rangle_t}{\rho [1 - B(t)]} \\ &\times [\langle R0 \rangle_t + \alpha \langle IO \rangle_t] + \frac{\alpha}{2} \frac{(1 - \alpha)^2}{1 - \rho} \frac{\langle OI \rangle_t \langle I1 \rangle_t \langle II \rangle_t \langle IO \rangle_t}{\rho^2 [1 - B(t)]^2} + \frac{1 - \alpha}{2(1 - \rho)\rho B(t)} \frac{\langle OI \rangle_t \langle IR \rangle_t \langle RI \rangle_t}{\rho [1 - B(t)]} [\langle R0 \rangle_t + \alpha \langle IO \rangle_t] \\ &+ \frac{\alpha}{2} \frac{1 - \alpha}{1 - \rho} \frac{\langle I1 \rangle_t \langle OI \rangle_t \langle II \rangle_t}{\rho^2 [1 - B(t)]^2} [\langle R0 \rangle_t + \alpha \langle IO \rangle_t] + \frac{\alpha}{4} \left(\frac{1 - \alpha}{1 - \rho} \right)^2 \frac{\langle IO \rangle_t \langle OI \rangle_t^2 \langle II \rangle_t}{\rho^2 [1 - B(t)]^2} [\langle R0 \rangle_t + \alpha \langle IO \rangle_t]. \end{aligned} \quad (16)$$

Equations (10) and (13)–(16) form a set of five equations for B , $\langle RR \rangle$, $\langle RI \rangle$, $\langle IR \rangle$, and $\langle II \rangle$. These equations form a five-dimensional dynamical system. To compare with simulation data, we solve for the stable fixed points numerically. Results for the mobility are shown in Fig. 1 as solid lines for different values of α and ρ . The analytical results are in good agreement with numerical data, showing that the decoupling approximation is sufficient to capture the essential features of the model. We have also checked the results of the two- and three-site spatial averages numerically and analytically, and it is found that the decoupling scheme gives qualitatively correct results for the spatial averages. Our method represents a systematic way of deriving mean field theories from microscopic consideration by following the time evolution of the system. The decoupling scheme of retaining two-site spatial averages is the minimal procedure to obtain qualitatively correct mobility and spatial averages involving longer strings of sites [18].

The $\alpha = 1$ case deserves further discussion. For $\alpha = 1$, Eq. (9) gives

$$B(t+1) = \frac{1}{\rho} [\langle 10 \rangle_t + \langle RR \rangle_t], \quad (17)$$

where $\langle 10 \rangle_t = \langle R0 \rangle_t + \langle I0 \rangle_t$. The spatial average $\langle RR \rangle_{t+1}$ can be obtained by setting $\alpha = 1$ in Eq. (13) to get

$$\langle RR \rangle_{t+1} = \frac{\langle 10 \rangle_t \langle 0R \rangle_t \langle RR \rangle_t}{(1-\rho)\rho B(t)} + \frac{\langle RR \rangle_t^2}{\rho B(t)}. \quad (18)$$

To form a closed set of equations, we work out the spatial averages $\langle 10 \rangle_{t+1}$ and $\langle 0R \rangle_{t+1}$ within the approximation of retaining two-site correlations to get

$$\langle 10 \rangle_t = \rho - \left(1 - \frac{\langle 10 \rangle_t}{\rho}\right) \left(\rho - \langle 10 \rangle_t + \frac{\langle 10 \rangle_t^2}{1-\rho}\right) \quad (19)$$

and

$$\langle 0R \rangle_{t+1} = \langle 10 \rangle_t + \frac{\langle 0R \rangle_t \langle RR \rangle_t}{\rho B(t)} - \frac{\langle 10 \rangle_t \langle 0R \rangle_t \langle RR \rangle_t}{(1-\rho)\rho B(t)}, \quad (20)$$

where we have used the relations stated in Eq. (11). The fixed points satisfy $B(t+1) = B(t) \equiv B$, $\langle 10 \rangle_{t+1} = \langle 10 \rangle_t \equiv y$, $\langle RR \rangle_{t+1} = \langle RR \rangle_t \equiv z$, and $\langle 0R \rangle_{t+1} = \langle 0R \rangle_t \equiv w$. Hence they satisfy the simultaneous equations

$$\rho B = y + z, \quad (21)$$

$$y = \rho - \left(1 - \frac{y}{\rho}\right) \left(\rho - y + \frac{y^2}{1-\rho}\right), \quad (22)$$

$$z = \frac{z^2}{\rho B} + \frac{wyz}{(1-\rho)\rho B}, \quad (23)$$

$$w = y + \frac{wz}{\rho B} - \frac{wyz}{(1-\rho)\rho B}. \quad (24)$$

From Eq. (22), the stable fixed point for y is given by $y = \rho$ for $\rho < 1/2$ and $y = 1 - \rho$ for $\rho \geq 1/2$. From Eq. (23), $z = 0$ is a stable fixed point for $\rho < 1/2$ and $z = \rho B - w$ is a stable fixed point for $\rho \geq 1/2$, where we have used the results for y . It is important to note that Eq. (24) for w becomes redundant. Hence the situation is that we have three equations with four unknowns. The values of B and z are governed by the linear relation

$$z = \rho B - (1 - \rho). \quad (25)$$

Any values of $B \in [(1-\rho)/\rho, 1]$ and $z \in [0, 2\rho - 1]$ satisfying Eq. (25) is a solution to the system of equations. Thus, for $\alpha = 1$, the mobility $B = 1$ for $\rho < 1/2$ and B lies in the range $[(1-\rho)/\rho, 1]$ for $\rho \geq 1/2$ with the precise value depending on the initial condition, in agreement with numerical results. The value $(1-\rho)/\rho$ shown in Fig. 1 corresponds to the initial condition of all the atoms being immobile.

B. Model B

The new parameter γ introduced in rule B1 is the probability that an atom in the running state changes into the immobile state in a time step. To carry out analytical treatments similar to those in model A, it is convenient to divide each time interval into two halves. In the first half of a time step, rule B1 applies and the parameter γ is effective, while in the second half of the time step, rules A1 and A2 apply. Introducing a Boolean variable $\zeta_{i,t}(\gamma)$ analogous to, but statistically independent of, $\theta_{i,t}(\alpha)$ and $\eta_{i,t}$, the variables $R_i(t)$ and $I_i(t)$ evolve in the first half of the time step as

$$R_i(t + \frac{1}{2}) = \overline{\zeta_{i,t}(\gamma)} R_i(t) \quad (26)$$

and

$$I_i(t + \frac{1}{2}) = I_i(t) + \zeta_{i,t}(\gamma) R_i(t). \quad (27)$$

The time evolution in the second half of the time step is given by Eqs. (5) and (6), with the quantities on the right-hand side of the equations corresponding to those evaluated at $t + 1/2$. Combining the evolution in the two halves of a time step, we finally arrive at

$$\begin{aligned} R_i(t+1) = & \{[\overline{\zeta(\gamma)} + \theta(\alpha)\zeta(\gamma)]R + \theta(\alpha)I\}_{i-1,t} [\overline{S}]_{i,t} [\overline{S} + (\zeta(\gamma) + \theta(\alpha)\zeta(\gamma))R + \theta(\alpha)I]_{i+1,t} \\ & + \{\eta(\frac{1}{2})[\overline{\zeta(\gamma)} + \theta(\alpha)\zeta(\gamma)]R + \eta(\frac{1}{2})\theta(\alpha)I\}_{i-1,t} [\overline{S}]_{i,t} [\overline{\theta(\alpha)\zeta(\gamma)}R + \overline{\theta(\alpha)I}]_{i+1,t} \\ & + [\overline{\eta(\frac{1}{2})\zeta(\gamma)}R]_{i,t} [\overline{S}]_{i+1,t} [\overline{\theta(\alpha)\zeta(\gamma)}R + \overline{\theta(\alpha)I}]_{i+2,t} + [\overline{\zeta(\gamma)}R]_{i,t} [\overline{\zeta(\gamma)}R]_{i+1,t} \end{aligned} \quad (28)$$

and

$$\begin{aligned}
I_i(t+1) = & \{ \overline{S} + [\zeta(\gamma) \overline{\theta(\alpha)} + \overline{\eta(\frac{1}{2})\zeta(\gamma)} + \overline{\eta(\frac{1}{2})\theta(\alpha)\zeta(\gamma)}]R + [\overline{\theta(\alpha)} + \overline{\eta(\frac{1}{2})\theta(\alpha)}]I \}_{i-1,t} [\overline{S}]_{i,t} [\overline{\theta(\alpha)\zeta(\gamma)R + \overline{\theta(\alpha)}I}]_{i+1,t} \\
& + [\overline{\eta(\frac{1}{2})\theta(\alpha)\zeta(\gamma)R + \overline{\eta(\frac{1}{2})\theta(\alpha)}I}]_{i,t} [\overline{S}]_{i+1,t} [\overline{\theta(\alpha)\zeta(\gamma)R + \overline{\theta(\alpha)}I}]_{i+2,t} + \{ [\overline{\eta(\frac{1}{2})\zeta(\gamma)} + \overline{\eta(\frac{1}{2})\theta(\alpha)\zeta(\gamma)}]R \\
& + \overline{\eta(\frac{1}{2})\theta(\alpha)}I \}_{i-2,t} [\overline{S}]_{i-1,t} [\overline{\theta(\alpha)\zeta(\gamma)R + \overline{\theta(\alpha)}I}]_{i,t} + [\overline{\theta(\alpha)\zeta(\gamma)R + \overline{\theta(\alpha)}I}]_{i,t} [\overline{S}]_{i+1,t} \\
& + [\overline{S}]_{i-1,t} [\overline{\theta(\alpha)\zeta(\gamma)R + \overline{\theta(\alpha)}I}]_{i,t} + [\overline{\zeta(\gamma)R}]_{i,t} [\overline{\zeta(\gamma)R + I}]_{i+1,t}. \tag{29}
\end{aligned}$$

Equations (28) and (29) are the time evolution equations relating $R_i(t+1)$ and $I_i(t+1)$ to quantities at time t . They play exactly the same role as Eqs. (5) and (6) in model A.

It is then straightforward to carry out the same treatment for model B as in model A, and we simply outline the key steps in the following discussion. Following the same steps leading to Eq. (9), the mobility $B(t+1)$ at time $t+1$ for model B is given by

$$\begin{aligned}
B(t+1) = & \frac{1}{\rho} \left\{ (1-\gamma)^2 \langle RR \rangle_t + (1-\gamma+\alpha\gamma) \langle R0 \rangle_t \right. \\
& + \alpha \langle I0 \rangle_t - \frac{\alpha}{2} (1-\alpha) [\langle IOI \rangle_t + \gamma \langle R0I \rangle_t \\
& \left. + \langle IOR \rangle_t + \gamma^2 \langle R0R \rangle_t \right\}. \tag{30}
\end{aligned}$$

Equation (30) is the generalization of Eq. (9) to model B. It reduces to Eq. (9) for $\gamma=0$. Employing a decoupling approximation to retain only spatial averages involving up to two nearest-neighboring sites, Eq. (30) becomes

$$\begin{aligned}
B(t+1) = & \frac{1}{\rho} \left\{ (1-\gamma)^2 \langle RR \rangle_t + (1-\gamma+\alpha\gamma) \langle R0 \rangle_t \right. \\
& + \alpha \langle I0 \rangle_t - \frac{\alpha}{2} \frac{1-\alpha}{1-\rho} [\langle IO \rangle_t + \gamma \langle R0 \rangle_t] \\
& \left. \times [\langle OI \rangle_t + \gamma \langle OR \rangle_t] \right\}. \tag{31}
\end{aligned}$$

To close the set of equations, we construct the time evolution equations for the spatial averages $\langle RR \rangle$, $\langle RI \rangle$, $\langle IR \rangle$, and $\langle II \rangle$. The other spatial averages can be constructed from these four averages. In the presence of the parameter γ , the resultant equations are more complicated than Eqs. (13)–(16) in model A. This set of equations forms a dynamical system. The stable fixed point corresponding to the mobility and spatial averages in the long-time limit can be readily solved numerically. Results for the mobility B in the steady state are shown as solid lines in Figs. 2 and 3 for two different values of atomic concentration ρ . The theoretical results obtained within the decoupling approximation capture all the essential features of the numerical data. It is observed that the theoretical results are consistently slightly greater than the numerical data. The discrepancies come from the decoupling scheme. If the decoupling approximation is extended to retain spatial averages involving up to three neighboring sites, for which the calculations are much more involved, the results are in better agreement with numerical data [19]. It is, however, important to stress that the essential physics is captured within the two-site decoupling approximation.

The particular case of $\alpha=1$ can be treated in a way analogous to that in model A. It is found that for $\gamma \in (0,1]$, the stable attractors give the mobility

$$B(t \rightarrow \infty) = \begin{cases} 1 & \text{if } \rho < 1/2, \\ \frac{1-\rho}{\rho} & \text{if } \rho \geq 1/2, \end{cases} \tag{32}$$

together with the spatial averages

$$\langle 10 \rangle_{t \rightarrow \infty} = \langle 0R \rangle_{t \rightarrow \infty} = \begin{cases} \rho & \text{if } \rho < 1/2, \\ 1-\rho & \text{if } \rho \geq 1/2, \end{cases} \tag{33}$$

and

$$\langle RR \rangle_{t \rightarrow \infty} = 0. \tag{34}$$

For $\alpha=1$ and $\gamma \neq 0$, the time evolution of the state at a site depends on the states of the nearest-neighboring sites only and hence the decoupling scheme retaining only two-site spatial averages is good. Results so obtained are in exact agreement with numerical data. It should be noted that for $\gamma=0$ and $\alpha=1$, $B=1$ for $\rho < 1/2$ and B lies in the range $[(1-\rho)/\rho, 1]$ for $\rho \geq 1/2$ with the precise value depending on the initial condition as discussed in the previous subsection.

IV. SUMMARY

In summary, we have proposed three CA models defined in terms of parallel updating rules analogous to the three models recently studied by Braun *et al.* [14] which are defined in terms of sequentially updating rules. These models are of increasing complexity so as to model the generalized FK models proposed recently within the context of tribology. The first model (model A) involves atoms in two different dynamical states, i.e., running and immobile, subjected to an external field parametrized by α . Atoms in the running state tend to hop along the field direction while atoms in the immobile state may bounce backward. The second model (model B) involves spontaneous transition of atoms from the running state to the immobile state in addition to the rules of model A. The third model (model C) takes into account of the crowding effect of the system as well. Results of numerical simulations indicate that the mobility, which is defined as the fraction of atoms in the running state, as a function of α for the three models exhibit phase transitions, jammings, and hysteresis. This interesting feature of hysteresis in model C can be understood qualitatively by noting the asymmetry in the formation of compact blocks of running atoms followed by compact blocks of immobile atoms from different initial configurations. The proposed CA models have the advantage that they can be treated as dynamical systems and analyzed

by the microscopic approach previously applied to analogous models of traffic flow problems [17]. For models A and B in which the state of a site is affected by the nearest and next-nearest neighbors, time evolution equations of the state of the sites can be explicitly written down. The mobility of the system at time $t+1$ can be expressed in terms of spatial averages at time t involving not more than three sites. By invoking an approximation which decouples the spatial averages into products of spatial averages involving up to two neighboring sites as well as deriving the evolution equations of the two-site spatial averages, a closed set of equations forming a nonlinear dynamical mapping can be established. The behavior in the long-time limit can be found by studying the stable fixed point of the mapping. The fixed point of the mapping can be found numerically. In the special case that $\alpha=1$ and $\gamma\neq 0$, the decoupling scheme is exact and analytical solutions can be found. For the whole range of possible values of the parameters in the models, the present approach yields satisfactory results when compared with simulation

data. Our analytical approach represents a systematic way to derive approximations of increasing accuracy starting from a microscopic point of view by following the time evolution of the system. It is expected that better agreement with numerical results can be obtained by retaining spatial averages involving a long string of neighboring sites.

ACKNOWLEDGMENTS

B.H.W. acknowledges support from the Chinese National Basic Research Climbing-up Project ‘‘Nonlinear Science,’’ and the National Natural Science Foundation in China. P.M.H. acknowledges support from the Research Grants Council (RGC) of the Hong Kong SAR Government under Grant No. CUHK 4191/97P. The work of B.H. and B.H.W. was also supported in part by grants from the Hong Kong Research Grants Council (RGC) and the Hong Kong Baptist University Faculty Research Grants (FRG). We thank Professor O. M. Braun for useful discussions.

-
- [1] See, for example, the articles in *Nonequilibrium Statistical Mechanics in One Dimension*, edited by V. Privman (Cambridge University Press, New York, 1997).
- [2] B. Schmittmann and R. K. P. Zia, in *Phase Transitions and Critical Phenomena*, edited by C. Domb and J. L. Leibowitz (Academic Press, San Diego, 1995), Vol. 17.
- [3] Y. Frenkel and T. Kontorova, *Phys. Z. Sowjetunion* **13**, 1 (1938).
- [4] I. F. Lyuksyutov, *Two-Dimensional Crystals* (Academic Press, Boston, 1992).
- [5] B. N. J. Persson, *Phys. Rev. Lett.* **71**, 1212 (1993).
- [6] F.-J. Elmer, *Phys. Rev. E* **50**, 4470 (1994); M. Weiss and F.-J. Elmer, *Phys. Rev. B* **53**, 7539 (1996).
- [7] M. G. Rozman, M. Urbakh, and J. Klafter, *Phys. Rev. Lett.* **77**, 683 (1996); *Europhys. Lett.* **39**, 183 (1997).
- [8] O. M. Braun, T. Dauxois, M. V. Paliy, and M. Peyrard, *Phys. Rev. Lett.* **78**, 1295 (1997); *Phys. Rev. E* **55**, 3598 (1997).
- [9] M. V. Paliy, O. M. Braun, T. Dauxois, and B. Hu, *Phys. Rev. E* **56**, 4025 (1997).
- [10] O. M. Braun, A. R. Bishop, and J. Roder, *Phys. Rev. Lett.* **79**, 3692 (1997).
- [11] K. Nagel and M. Schreckenberg, *J. Phys. I* **2**, 2221 (1992); M. Schreckenberg, A. Schadschneider, K. Nagel, and N. Ito, *Phys. Rev. E* **51**, 2939 (1995).
- [12] M. Fukui and Y. Ishibashi, *J. Phys. Soc. Jpn.* **65**, 1868 (1996).
- [13] K. H. Chung, P. M. Hui, and G. Q. Gu, *Phys. Rev. E* **51**, 772 (1995); B. H. Wang, Y. F. Woo, and P. M. Hui, *J. Phys. A* **29**, L31 (1996); B. H. Wang and P. M. Hui, *J. Phys. Soc. Jpn.* **66**, 1238 (1997).
- [14] O. M. Braun, B. Hu, A. Filippov, and A. Zelster, *Phys. Rev. E* **58**, 1311 (1998).
- [15] B. Derrida, E. Domany, and D. Mukamel, *J. Stat. Phys.* **69**, 667 (1992); B. Derrida, M. R. Evans, V. Hakim, and V. Pasquier, *J. Phys. A* **26**, 1493 (1993); G. Schütz and E. Domany, *J. Stat. Phys.* **72**, 277 (1993).
- [16] A. Schadschneider and M. Schreckenberg, *J. Phys. A* **30**, L69 (1997).
- [17] B. H. Wang, Y. R. Kwong, and P. M. Hui, *Phys. Rev. E* **57**, 2568 (1998); *Physica A* **254**, 122 (1998).
- [18] Y. R. Kwong, P. M. Hui, and B. H. Wang (unpublished). While the simplest decoupling to obtain the mobility is to ignore any spatial correlations so that only one-site spatial averages are retained, it can be shown that although the mobility so obtained is in reasonable agreement with numerical data, the two-site spatial averages are qualitatively incorrect.
- [19] Y. R. Kwong (unpublished). When the effects of three-site spatial correlations are included, the agreement between theory and numerical data is slightly improved.